CHIN. PHYS. LETT. Vol. 38, No. 1 (2021) 017201

Temperature Dependent In-Plane Anisotropic Magnetoresistance in $HfTe_5$ Thin Layers

Peng Wang(王鹏)[1,2†], Tao Hou(侯涛)[1†], Fangdong Tang(汤方栋)[2,3], Peipei Wang(王培培)[2], Yulei Han(韩玉磊)[1], Yafei Ren(任亚飞)[1], Hualing Zeng(曾华凌)[1*], Liyuan Zhang(张立源)[2*], and Zhenhua Qiao(乔振华)[1*]

[1]*International Center for Quantum Design of Functional Materials, Hefei National Laboratory for Physical Sciences at the Microscale, Synergetic Innovation Centre of Quantum Information and Quantum Physics, CAS Key Laboratory of Strongly Coupled Quantum Matter Physics, and Department of Physics, University of Science and Technology of China, Hefei 230026, China*

[2]*Department of Physics, Southern University of Science and Technology, and Shenzhen Institute for Quantum Science and Engineering, Shenzhen 518055, China*

[3]*Solid State Nanophysics, Max Plank Institute for Solid State Research, Stuttgart, Germany*

(Received 18 October 2020; accepted 18 November 2020; published online 6 January 2021)

We report the observation of in-plane anisotropic magnetoresistance and planar Hall effect in non-magnetic $HfTe_5$ thin layers. The observed anisotropic magnetoresistance as well as its sign is strongly dependent on the critical resistivity anomaly temperature T_p. Below T_p, the anisotropic magnetoresistance is negative with large negative magnetoresistance. When the in-plane magnetic field is perpendicular to the current, the negative longitudinal magnetoresistance reaches its maximum. The negative longitudinal magnetoresistance effect in $HfTe_5$ thin layers is dramatically different from that induced by the chiral anomaly as observed in Weyl and Dirac semimetals. One potential underlying origin may be attributed to the reduced spin scattering, which arises from the in-plane magnetic field driven coupling between the top and bottom surface states. Our findings provide valuable insights for the anisotropic magnetoresistance effect in topological electronic systems and the device potential of $HfTe_5$ in spintronics and quantum sensing.

DOI: 10.1088/0256-307X/38/1/017201

Negative longitudinal magnetoresistance (NLMR) has been intensively observed in ferromagnetic metals[1–3] with structural anisotropy.[4–7] For this type of NLMR, one origin is the external-field-induced magnetization that reduces the carrier spin scattering and thereby increases the conductivity in electric transport. Nevertheless, in conventional metallic ferromagnets, the NLMR effect is relatively weak and there are too many impurities in material systems, limiting their practical applications in memory or sensing. Recently, large NLMR effect resulted from chiral anomaly was verified in topological electronic systems, e.g., Dirac and Weyl semimetals.[8–12] However, due to the required chiral charge pumping between separated Weyl nodes, it requests subtle direction alignment of the applied external magnetic field and electric field. The experimental realization of noticeable NLMR in topological materials is still challenging. Therefore, seeking other NLMR effect is of fundamental importance for the integration of topological materials in electronics.

In this Letter, we report our observation of anisotropic magnetoresistance (AMR) in $HfTe_5$ thin layers with the sign controlled by temperature, which allows to generate large and magnetic-field direction insensitive NLMR effect. $HfTe_5$ is a layered topological material with a unique lattice structure:[13] the one-dimensional atomic chain $HfTe_3$ extends along the a direction together with two tellurium atoms connecting the chains into a plane in c direction, and then stacking in b direction to form the bulk, where a, b, and c directions are set to be x, z, and y axes as shown in Fig. 1(a). Because of the weak bonding strength along the b and c directions, the lattice constants respond differently to temperature. Therefore, $HfTe_5$ is considered as either a strong or weak topological insulator,[14] depending on the specific lattice constants. In contrast to bulk systems, where the NLMR

Supported by the National Key R&D Program (Grant Nos. 2017YFB0405703, 2017YFA0205004, and 2018YFA0306600), and the National Natural Science Foundation of China (Grant Nos. 11974327, 11474265, 11674295, 11674024, and 11874193), the Fundamental Research Funds for the Central Universities (Grant Nos. WK2030020032 and WK2340000082), Anhui Initiative in Quantum Information Technologies, and the Shenzhen Fundamental Subject Research Program (Grant No. JCYJ20170817110751776). This work was partially carried out at the USTC Center for Micro and Nanoscale Research and Fabrication.

†Peng Wang and Tao Hou contributed equally to this work.

*Corresponding authors. Email: hlzeng@ustc.edu.cn; zhangly@sustech.edu.cn; qiao@ustc.edu.cn

effect is induced by chiral anomaly,[12,15] the origin of in-plane NLMR effect in the system of $HfTe_5$ thin layers is completely different. At cryogenic temperature, the NLMR is observed in most of the in-plane field directions. The magnitude of this NLMR effect can reach up to 30%, which is much higher than that in the conventional ferromagnets.

In experiment, the electronic transport measurements were performed in $HfTe_5$ thin layers with tens of nanometers. We observed temperature-dependent in-plane AMR. The anisotropy reverses around the critical resistivity anomaly temperature T_p. Below T_p, the positive magnetoresistance turns to be negative at most of the in-plane field directions. The NLMR reaches the maximum when the in-plane magnetic field is perpendicular to current, which rules out the origin of chiral anomaly in our study. By measuring the angle and temperature dependence of magnetoresistance, we found that the formation of the Landau levels inhibits the NLMR effect at low temperature and strong magnetic field. In addition, the correlation between the sign reverse temperatures of AMR and T_p suggests that the appearance of the AMR and the NLMR is related to the band structure near the Fermi energy. According to these evidences, we found one origin of these phenomena, i.e., the in-plane magnetic field can shift the Dirac point in k space, and the hybrid coupling between top and bottom surface states can generate angle-dependent net spin polarization that can induce anisotropy and reduce the spin scattering.[16,17]

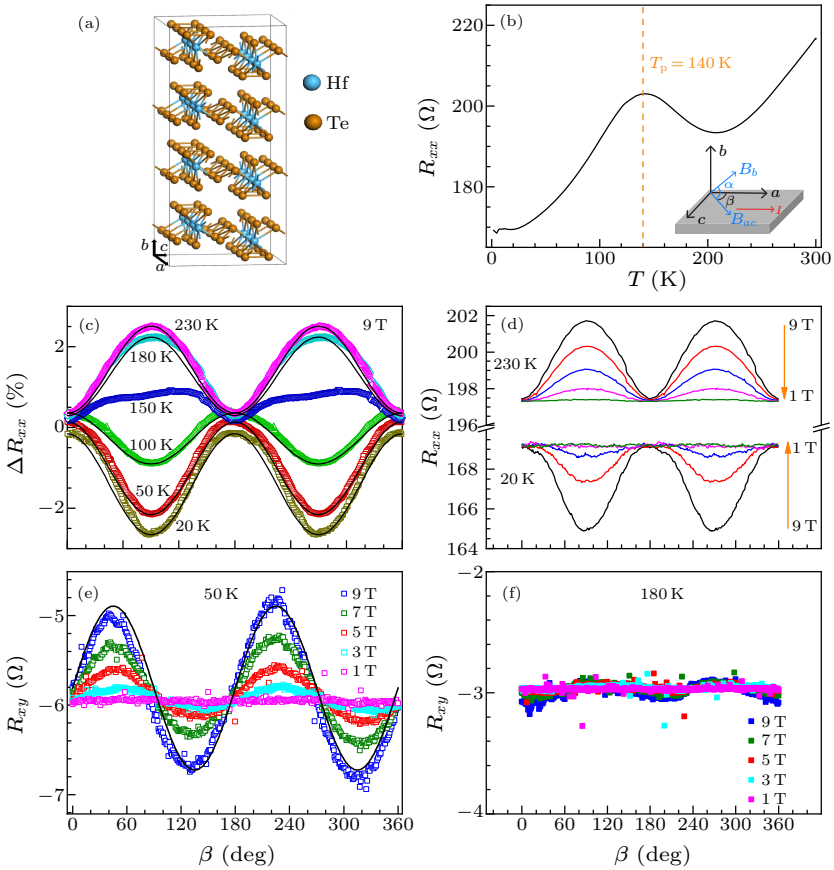

Fig. 1. In-plane anisotropic longitudinal and Hall resistance of $HfTe_5$ thin layers. (a) Crystal structure of $HfTe_5$. (b) Temperature-dependent longitudinal resistance of $HfTe_5$. The peak temperature is marked by the dashed line at about 140 K. The inset is schematic of the transport measurements. The current is always along a direction and the magnetic field rotates in ab and ac planes labeled by α and β. (c) In-plane anisotropic magnetoresistance R_{xx} at different temperatures from 20 K to 230 K under 9 T. The black lines are the fitting according to $R_{xx} = R_\perp - \Delta R \times \cos^2\beta$, $\Delta R = R_\perp - R_\parallel$. (d) High (230 K) and low (20 K) temperature anisotropic magnetoresistance under different magnetic fields: 1 T, 3 T, 5 T, 7 T, and 9 T. (e) and (f) Planar Hall effect at 50 K and 180 K under different magnetic fields. Due to the misalignment between the sample and magnetic field, the base line is not zero after symmetrization.

In the sample preparation, we took 99.999% Hf powder and Te powder to grow single crystal of $HfTe_5$ using the chemical vapor transport method, then mechanically dissociated the bulk with scotch tape and poly dimethyl siloxane (PDMS). There will be some thin-layer samples on the PDMS in about dozens of nanometers. We transferred them to a silicon wafer with 280 nm SiO_2 surface and made a six-electrode

pattern by electron beam lithography. The mobility of the $HfTe_5$ thin layers is about 10000, which is an order of magnitude less than the bulk sample, and the carrier density is about $1.0 \times 10^{18}\,\mathrm{cm}^{-3}$, which is about an order of magnitude higher than the bulk sample. We find that the properties of the samples from different batches are slightly different, whereas the NLMR effect always exists.

The in-plane AMR measurement was performed in a physical property measurement system. The temperature range was 2–300 K, the magnetic field range was 0–14 T, and the rotation angle range was 0–360°. The remaining experimental items were measured in the TeslatronPT Dewar of Oxford Instrument of SUST, where the temperature range was 1.5–300 K, and the magnetic field range was 0–13 T. During the measurement, the current was always along a direction, and the magnetic field rotated along the ab and ac planes, which are denoted by α and β, respectively, as shown in the inset of Fig. 1(b).

The in-plane AMR was observed in $HfTe_5$ thin layers, where the magnetoresistance is defined as $\Delta R_{xx} = \frac{R_{xx}(B)-R_{xx}(0\,T)}{R_{xx}(0\,T)}$. Figure 1(c) shows the temperature dependence of AMR. The obvious AMR signals can be found under high magnetic fields even at room temperature. The conventional fitting formula of AMR can be written as[6]

$$\begin{aligned} R_{xx} &= R_\perp - \Delta R \cos^2\alpha, \\ \Delta R &= R_\perp - R_\parallel, \end{aligned} \tag{1}$$

where $R_\perp(R_\parallel)$ represents the longitudinal resistance when the in-plane magnetic field is perpendicular (parallel) to the current. We have fitted the curves at different temperatures according to Eq. (1), as shown in Fig. 1(c) by black lines. One can find that the measured data relatively coincide with the fitted curves at various temperatures. There are two reasons for the slightly deviating parts: (i) The sample placement is not exactly parallel to the magnetic field, and the out-of-plane magnetoresistance components are mixed in the data, which can be proved by the analysis of Hall effect R_{xy}. (ii) We have performed symmetry analysis on the data to remove the Hall component by adding the data under positive and negative magnetic field, but this operation cannot cancel the planar Hall resistance, so that the planar Hall resistance is also mixed in the data, making the data deviate from the fitting. The data at 150 K is obviously different from the others and the inversion of anisotropy also occurs near this temperature: $\Delta R = R_\perp - R_\parallel > 0$ at higher temperatures while $\Delta R = R_\perp - R_\parallel < 0$ at lower temperatures. We find that this phenomenon is closely related to the temperature-dependent resistance peak T_p of $HfTe_5$, as shown in Fig. 1(b), because the peak temperature of 140 K is close to the anisotropy inversion temperature. In addition, in the temperature range of $\Delta R = R_\perp - R_\parallel < 0$, the NLMR effect occurs in most of the in-plane directions and reaches the maximum at the perpendicular direction of $\beta = 90°$, which is completely different from the NLMR effect induced by chiral anomaly.[11,12] Figure 1(d) shows the magnetic field dependences of AMR at high temperature (230 K) and at low temperature (20 K). The AMR under different magnetic fields agrees with Eq. (1), and the higher the magnetic field, the larger the AMR.

Furthermore, we also study the variation of the Hall resistance R_{xy} around the inversion temperature. The raw data can be found in Section I of the Supplementary Materials. Hall magnetoresistance shows obvious sinusoidal dependence, which means that the sample is not exactly parallel to the magnetic field. There will be a sinusoidal out-of-plane perpendicular magnetic field component during rotation, thus the Hall signal varies sinusoidally with the angle. Adding the positive and negative fields' data can remove the Hall resistance brought by the out-of-plane magnetic field. However, the base line of Hall magnetoresistance is not at zero because some longitudinal signals are inevitably doped in the data. The whole analysis procedure can be found in Section I of the Supplementary Materials. Figures 1(e) and 1(f) show the Hall magnetoresistance at 50 K and 180 K, respectively. It can be found that there is a significant sinusoidal Hall resistance at low temperature, but not at high temperature. The conventional fitting formula of the planar Hall resistance can be written as

$$R_{xy} = -\Delta R_\mathrm{H} \sin\alpha \cos\alpha. \tag{2}$$

The black fitting line in Fig. 1(e) shows that the data fits well, indicating that the Hall signal is actually the planar Hall resistance. It is worth mentioning that the parameters in fittings of Eqs. (1) and (2) are different, i.e., $\Delta R_\mathrm{H} \neq \Delta R$, implying that the planar Hall effect may be induced by multiple reasons.

Next, we study the angle dependence of negative longitudinal magnetoresistance. When the temperature is lower than the inversion temperature, we could observe the in-plane NLMR in $HfTe_5$ thin layers. Since the signal itself can arise from an extrinsic origin, i.e., current jetting[18] that is a measurement error caused by the non-uniform distribution of current, we first confirm the source of the NLMR using a special electrode structure in sample S7. We prepare a six-electrode pattern and make sure that the electrodes completely vertically go across the sample, ensuring that the measured signals are not affected by the uneven current distribution (see detailed information in Section Ⅱ of the Supplementary Materials). One can find that the NLMR effect can still be measured in this sample, and both angle and temperature

variation trends are completely consistent with those of the ordinary sample, indicating that the NLMR signal is an intrinsic characteristic of the sample itself, rather than the measurement error.

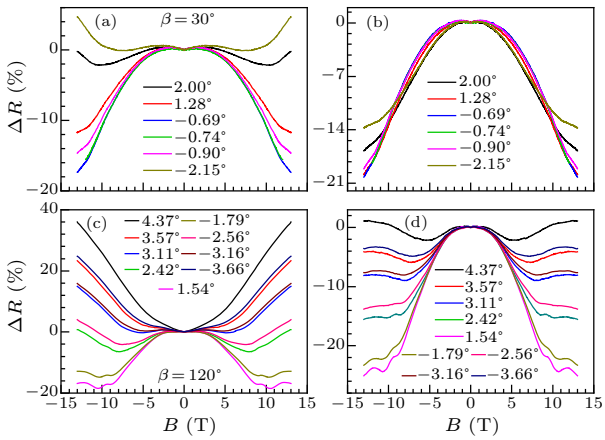

Fig. 2. Out-of-plane magnetic field dependence of NLMR effect of $HfTe_5$ with $\Delta R = \frac{R(B)-R_0}{R_0}$. (a) The α dependence of magnetoresistance from 2.00° to −2.15° when we fix $\beta = 30°$. (b) The data after subtracting the b direction component according to different α from (a). (c) The α dependence of magnetoresistance from 4.37° to −3.66° when we fix $\beta = 120°$. (d) The data after subtracting the b direction component according to different α from (c).

Then, we carefully study the angle and temperature dependences of the NLMR effect. In some samples, the amplitude of NLMR can reach tens of percent, which is much higher than those in some common ferromagnetic materials. Figure 2(a) shows the α dependence of NLMR. The magnetic field is mainly placed in plane with $\beta = 30°$, and it slightly deviates from the plane by a small angle α. The precise angle α in the figure comes from the Hall measurements. By comparing the magnetic fields with the same Hall resistance between in-plane and out-of-plane directions, one can determine the component of the magnetic field offset in b direction and calculate the α angle. The detailed calculation method is provided in Section Ⅲ of the Supplementary Materials. Figure 2(a) shows that as the out-of-plane component increases, the NLMR quickly disappears. A small angular offset can induce a large positive magnetoresistance component that covers the NLMR signal, because of the large positive magnetoresistance of $HfTe_5$ in b direction. Since the deflection angle α is small and the sample is very anisotropic, we can treat the total magnetoresistance as the vector sum of the in-plane and out-of-plane magnetoresistances. By subtracting the b direction component, one can get the in-plane component shown in Fig. 2(b). All the curves with different deflection angles are coincident, confirming that the NLMR signal is indeed caused by the in-plane magnetic field.

When changing the in-plane magnetic field to $\beta =$ 120°, as shown in Fig. 2(c), we can find some similar characteristics, i.e., the positive magnetoresistance component outside the plane will cover the NLMR signal, and after the component in b direction is subtracted, the curves are partly coincident, as shown in Fig. 2(d). The data are only overlapped in the low magnetic field, whereas the NLMR signal is greatly suppressed in high magnetic field due to the SdH oscillations. This indicates that when the Landau levels are formed in the presence of high magnetic field, the NLMR effect becomes obviously suppressed, implying that the existence of NLMR effect may be related to the band structure near the Fermi energy.

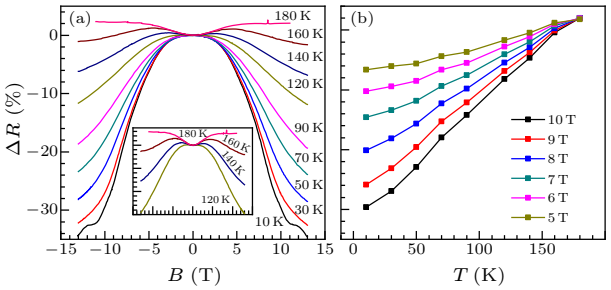

Fig. 3. Temperature-dependent negative longitudinal magnetoresistance of $HfTe_5$. (a) Temperature dependence of negative longitudinal magnetoresistance from 10 K to 180 K, where $\alpha = 0°$, $\beta = 75°$. The inset gives the zoom-in display at high temperatures from 120 K to 180 K, where negative and positive magnetoresistance coexist. (b) The temperature dependence of amplitude of magnetoresistance ΔR under different magnetic fields.

Now we continue to study the effect of temperature on NLMR effect, i.e., temperature dependence of negative longitudinal magnetoresistance, as shown in Fig. 3(a). When the magnetic field is applied in different in-plane directions, it shows the same variation trend, i.e., as the temperature increases, the amplitude of the NLMR gradually decreases. However, it always keeps a good NLMR profile till reaching the inversion temperature. Below the inversion temperature, the NLMR effect will be more obvious in higher magnetic field at lower temperature, as shown in Fig. 3(b). Above the inversion temperature, the negative longitudinal magnetoresistance is gradually replaced by the positive magnetoresistance from low to high field. When the temperature reaches ∼180 K, the NLMR effect completely disappears. In bulk $HfTe_5$, the angular resolution photoelectron spectroscopy (ARPES) and transport measurements suggest that the Fermi level can shift from the valence band to conduction band as the temperature decreases, and the Fermi level will go through Dirac point at temperature T_p, so that the correlation between the critical temperature of the NLMR and T_p confirms again that the existence of NLMR is closely related to the special band structures. It is noteworthy

that we do not find distinct evidences for the transition of Fermi energy by transform measurements in the thin layers' system. In the range of 2–300 K, the major carriers are always holes (see Section Ⅳ of the Supplementary Materials). In following study, if the Fermi energy in the thin-layer system shares the same transition tendency as the bulk, it is expected to be experimentally verified by ARPES measurements.

Summarizing the experimental results, we can find that the inversion of AMR, and the appearance of planar Hall effect and NLMR effects are all related to the resistivity anomaly temperature $T_{\rm p}$. Meanwhile, the formation of Landau levels also strongly suppresses the NLMR effect. Therefore, we attribute the appearance of these phenomena to the topological electronic band structures of $HfTe_5$. According to some similar experimental phenomena,[16,17,19,20] we believe that the temperature dependent anisotropy and the NLMR effect could be induced by the hybrid coupling of surface states, in which the carriers are spin-momentum locked. The Dirac-like surface electronic band structure is displayed in Fig. 4(a). When an in-plane magnetic field is applied, a momentum shift occurs in the band structure of the top and bottom surface states. Therefore, the top and bottom surfaces will hold two kinds of carriers with completely opposite spin polarizations. When the sample is thin enough, the hybrid coupling between the top and bottom surface states can generate a net spin polarization $S_{\rm net}$, which can suppress the spin scattering and induce negative longitudinal magnetoresistance, as shown in Fig. 4(b). Different directions of in-plane magnetic field can change the net spin directions, resulting in AMR. In addition, when the Fermi level lies in the conduction band or valence band, the directions of $S_{\rm net}$ are opposite, corresponding to the inversion of AMR around $T_{\rm p}$.

Furthermore, we find that the NLMR only exists in the samples with thickness of tens of nanometers, as shown in Table 1. In thick samples, the coupling between surface states becomes weaker, so that the NLMR effect disappears, which can be verified in samples S8, S9 and S10. Although the NLMR effect should be more pronounced in thinner samples, we do not observe it in thinner samples S1 and S2. We also find that the temperature-dependent longitudinal resistance peak $T_{\rm p}$ disappears in these thinner samples (see detailed information in Section V of the Supplementary Materials). Usually, the Fermi energy slightly rises as the temperature decreases. Therefore, the absence of $T_{\rm p}$ indicates that the Fermi energy is deeply located inside the valence band. Consequently, the bulk states are dominant in electrical transport, and covering the negative longitudinal magnetoresistance.

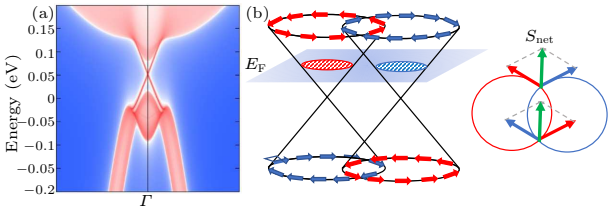

Fig. 4. The schematic diagram of AMR and NLMR effect. (a) The topological surface states of $HfTe_5$ (001) plane. (b) Shifted band structure of top and bottom surface states under in-plane magnetic field and the generation of net spin polarization $S_{\rm net}$. The red and blue arrows represent the spin polarization direction.

Table 1. Negative longitudinal magnetoresistance in different thickness samples.

Sample thickness	Abnormal cooling peak $T_{\rm p}$	Negative magnetoresistance ($B \parallel c$ axis)
S1-16 nm	No	No
S2-25 nm	No	No
S3-28 nm	Yes	Yes
S4-35 nm	Yes	Yes
S5-38 nm	Yes	Yes
S6-51 nm	Yes	Yes
S7-60 nm	Yes	Yes
S8-88 nm	Yes	No
S9-100 nm	Yes	No
S10-330 nm	Yes	No

In conclusion, we have observed distinctive electrical transport phenomena in non-magnetic $HfTe_5$ thin layers, e.g., in-plane anisotropic magnetoresistance, planar Hall effect and negative longitudinal magnetoresistance effect. In some samples, the amplitude of NLMR can reach tens of percent, which is much higher than those in common ferromagnetic materials, such as iron, cobalt, nickel and their alloys. All these effects are found to be related to the resistivity anomaly $T_{\rm p}$. Especially, the in-plane AMR reverses around temperature $T_{\rm p}$. The corresponding physical origin of these effects can be attributed to the hybrid coupling of surface states that produces a net polarized spin $S_{\rm net}$ in the presence of in-plane magnetic field, thus leading to anisotropic spin scattering and reducing the resistance.

References

[1] Shon W, Rhyee J S, Jin Y and Kim S J 2019 *Phys. Rev. B* **100** 24433

[2] Liu Z H, Liu H, Zhang X X, Zhang X K, Xiao J Q, Zhu Z Y, Dai X F, Liu G D, Chen J L and Wu G H 2005 *Appl. Phys. Lett.* **86** 182507

[3] Hanasaki N, Tajima H, Matsuda M, Naito T and Inabe T 2000 *Phys. Rev. B* **62** 5839

[4] Philippi-Kobs A, Farhadi A, Matheis L, Lott D, Chuvilin A and Oepen H P 2019 *Phys. Rev. Lett.* **123** 137201

[5] Kriegner D, Výborný K, Olejník K, Reichlová H, Novák V, Marti X, Gazquez J, Saidl V, Němec P, Volobuev V V, Springholz G, Holý V and Jungwirth T 2016 *Nat. Commun.* **7** 11623

[6] Mcguire T R and Potter R I 1975 *IEEE Trans. Magn.* **11** 1018

[7] Thomsom W 1857 *Proc. R. Soc. London* **8** 550

[8] Li C Z, Wang L X, Liu H, Wang J, Liao Z M and Yu D P 2015 *Nat. Commun.* **6** 10137

[9] Xiong J, Kushwaha S K, Liang T, Krizan J W, Hirschberger M, Wang W, Cava R J and Ong N P 2015 *Science* **350** 413

[10] Huang X, Zhao L, Long Y, Wang P, Chen D, Yang Z, Liang H, Xue M, Weng H, Fang Z and O 2015 *Phys. Rev. X* **5** 031023

[11] Li Q, Kharzeev D E, Zhang C, Huang Y, Pletikosić I, Fedorov A V, Zhong R D, Schneeloch J A, Gu G D and Valla T 2016 *Nat. Phys.* **12** 550

[12] Wang H, Li C K, Liu H, Yan J, Wang J, Liu J, Lin Z, Li Y, Wang Y, Li L, Mandrus D, Xie X C, Feng J and Wang J 2016 *Phys. Rev. B* **93** 165127

[13] Hansson M, Brattås L, Kjekshus A, Enzell C R, Enzell C R and Swahn C G 1973 *Acta Chem. Scand.* **27** 2455

[14] Fan Z, Liang Q F, Chen Y B, Yao S H and Zhou J 2017 *Sci. Rep.* **7** 1

[15] Zhao L X, Huang X C, Long Y J, Chen D, Liang H, Yang Z H, Xue M Q, Ren Z A, Weng H M, Fang Z, Dai X and Chen G F 2017 *Chin. Phys. Lett.* **34** 037102

[16] Sulaev A, Zeng M, Shen S Q, Cho S K, Zhu W G, Feng Y P, Eremeev S V, Kawazoe Y, Shen L and Wang L 2015 *Nano Lett.* **15** 2061

[17] Zhang M, Wang H, Mu K, Wang P, Niu W, Zhang S, Xiao G, Chen Y, Tong T, Fu D, Wang X, Zhang H, Song F, Miao F, Sun Z, Xia Z, Wang X, Xu Y, Wang B, Xing D and Zhang R 2018 *ACS Nano* **12** 1537

[18] dos Reis R D, Ajeesh M O, Kumar N, Arnold F, Shekhar C, Naumann M, Schmidt M, Nicklas M and Hassinger E 2016 *New J. Phys.* **18** 085006

[19] Xu Y, Jiang G, Miotkowski I, Biswas R R and Chen Y P 2019 *Phys. Rev. Lett.* **123** 207701

[20] Taskin A A, Legg H F, Yang F, Sasaki S, Kanai Y, Matsumoto K, Rosch A and Ando Y 2017 *Nat. Commun.* **8** 1340

Supplementary Materials: Temperature dependent in-plane anisotropic magnetoresistance in $HfTe_5$ thin layers

Peng Wang(王鹏)[1,2,#], Tao Hou(侯涛)[1,#], Fangdong Tang(汤方栋)[2,3], Peipei Wang(王培培)[2], Yulei Han(韩玉磊)[1], Yafei Ren(任亚飞)[1], Hualing Zeng(曾华凌)[1,†], Liyuan Zhang(张立源)[2,†], Zhenhua Qiao(乔振华)[1,†]

1 International Center for Quantum Design of Functional Materials, Hefei National Laboratory for Physical Sciences at the Microscale, Synergetic Innovation Centre of Quantum Information and Quantum Physics, CAS Key Laboratory of Strongly Coupled Quantum Matter Physics, and Department of Physics, University of Science and Technology of China, Hefei, Anhui 230026, China.

2 Department of Physics, Southern University of Science and Technology, and Shenzhen Institute for Quantum Science and Engineering, Shenzhen, 518055, China

3 Solid State Nanophysics, Max Plank Institute for Solid State Research, Stuttgart, Germany.

[#] These authors contribute equally to this work.

[†] Corresponding authors: hlzeng@ustc.edu.cn, zhangly@sustc.edu.cn, and qiao@ustc.edu.cn

Section I: Data processing of planar Hall effect

Due to slightly unparallel between the sample and the magnetic field , a small amount of out-of-plane magnetic field component that changes sinusoidally with the angle β is doped into the data, which in turn produces a sinusoidally varying Hall resistance, shown as the red and blue lines in Fig. S1(a). By combining the Hall data under the same intensity of positive and negative magnetic fields, we can remove the out-of-plane Hall component, thereby obtaining a pure planar Hall effect resistance, shown as the green line in the Fig. S1(a). An obvious planar Hall effect with a period of π appears, but this symmetry analysis inevitably imports a small amount of longitudinal resistance, which shifts the baseline from 0. According to the plane Hall effect formula:

$$R_{xy} = -\Delta R_H \times \sin\alpha \times \cos\alpha \quad (1)$$

we find that the fitting is relatively coincident with the green line, indicating that the data showed in green line describe the planar Hall effect. Figure S1(b) shows the raw data of the Hall effect measured under different in-plane magnetic field. Through the same processing method, we get Fig. 1(e) in the text.

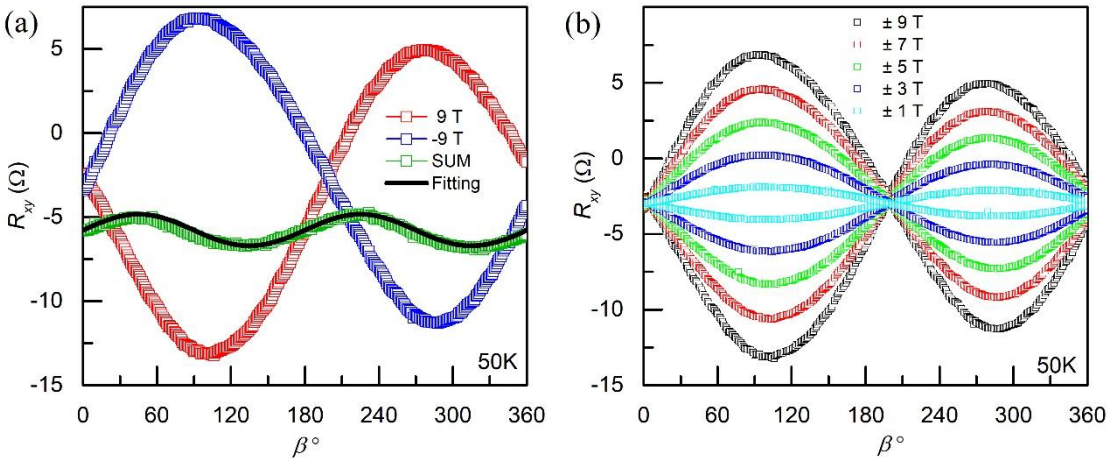

FIG. S1. In-plane angle-dependent Hall signal and planar Hall effect. (a) The planar Hall effect resistance (green line) obtained by symmetrization. The blue and red line are the raw data at 9 T and -9 T, and the black line is the fitting according to Equation (1). (b) The raw data of Hall signal under different in-plane magnetic fields.

Section II: Eliminating the extrinsic origin of negative longitudinal magnetoresistance

In order to confirm whether the negative longitudinal magnetoresistance is intrinsic or extrinsic (current jetting), we apply specific electrodes pattern onto the sample S7, as shown in Fig. S2(a), where all the electrodes completely vertically go across the sample, assuring the same potential. So that the measured signal will not be affected by uneven current distribution in this sample. And the same angle and temperature dependence of negative longitudinal magnetoresistance are also observed in sample S7, as shown in Fig. S2(b) and S2(c).

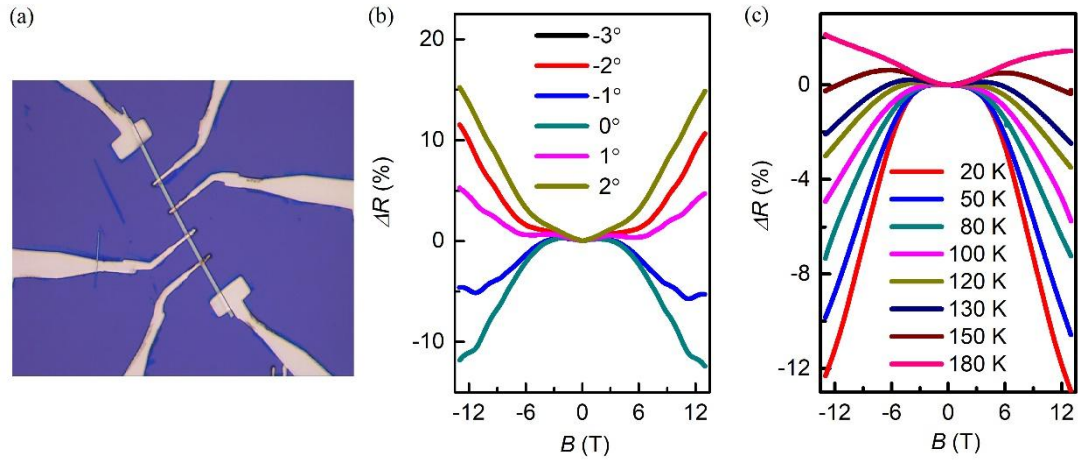

FIG. S2. Negative longitudinal magnetoresistance in the sample with homogeneous current distribution. (a) The microscope pattern of the sample S7. (b) Out-of plane angle-dependent negative longitudinal magnetoresistance where the magnetic fields mostly lie in *ac* plane with $\beta = 30°$, and slightly deviates with $\alpha = -3°, -2°, -1°, 0°, 1°, 2°$. (c) Temperature-dependent negative longitudinal magnetoresistance from 20 K to 180 K where the magnetic field is fixed in $\alpha = 0°, \beta = 30°$.

Section III: Detecting deflection angle α by Hall resistance

We calculate the detailed angle α in Fig. 2 by comparing the Hall resistance between out-of-plane perpendicular Hall resistance and in-plane Hall resistance. In Figure S3, the slope is contrary for the angle α with different sign. As the red line with $\alpha = 3.66°$, when in-plane magnetic field reaches 13 T, the Hall resistance is about 93 Ω which is all from the deviated (out-of-plane) component of magnetic field. We find that in Fig. S3(b), when magnetic field is out-of-plane perpendicular to the current, the same 93 Ω Hall resistance realizes at 0.83 T which equals to the deviated component mentioned when the magnetic field is in plane. So that we can infer the

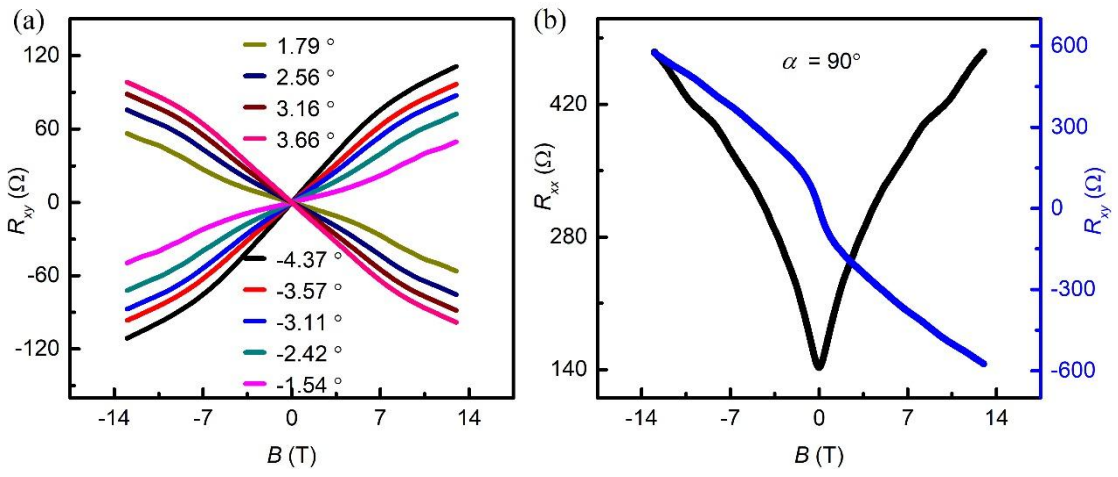

precise α from the trigonometric function $\alpha = \arcsin\left(\frac{0.83\ \mathrm{T}}{13\ \mathrm{T}}\right) = 3.66°$. The other precise angles in Fig.S3(a) are deduced by the same method.

FIG. S3. Comparison of Hall resistance between in-plane and out-of-plane magnetic field. (a) In-plane Hall measurement where the Hall resistance is from the deviated (out-of-plane) component of the magnetic field. The legends are deflection angles α. (b) Out-of-plane longitudinal and Hall measurements.

Section IV: Temperature dependence of longitudinal and Hall resistance

In thin-layers samples around dozens of nanometers, the Hall slope is always positive rather than inversing around temperature T_p, as shown in Fig. S4(b). We notice that the Hall resistance changes from linear to nonlinear when decreasing the temperature, which means that there might be more than one kind of carriers participating the transport process. This could be caused by the shift of Fermi level during decreasing the temperature. But we still can not conclude that the Fermi level goes through Dirac point at T_p by transport measurements. Whether the process occurs in thin-layers samples still needs further exploration and research, such as

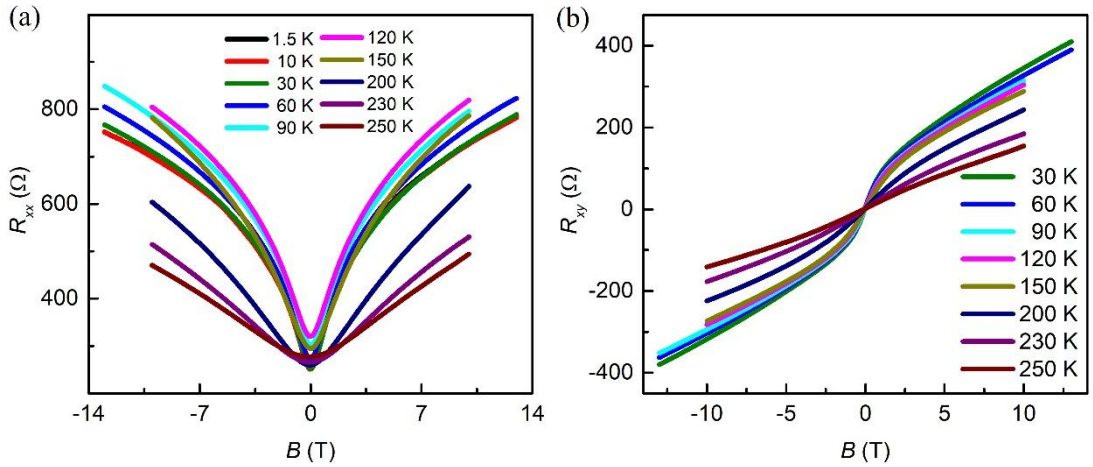

ARPES.

FIG. S4. Temperature-dependent longitudinal and Hall measurements. (a) Longitudinal magnetoresistance measurements under different temperature. (b) Hall measurements under different temperature. It shows that the slope is always positive under different temperature which is different from the bulk samples that the slope is

inversed at T_p.

Section V: Electrical transport measurement of samples with different thicknesses

In both thicker and thinner samples, we have not observed the in-plane NLMR, as shown in Fig. S5 (b). The resistivity anomaly peak T_p of $HfTe_5$ indicates that the Fermi surface goes through the Dirac point. By comparing the temperature dependent resistance of samples with different thicknesses, we find that as the thickness decreases, T_p gradually disappears, indicating that the Fermi energy may be deeply located inside the valence band. So that the system mainly exhibits the transport properties of bulk states at this time, and the NLMR effect cannot be observed.

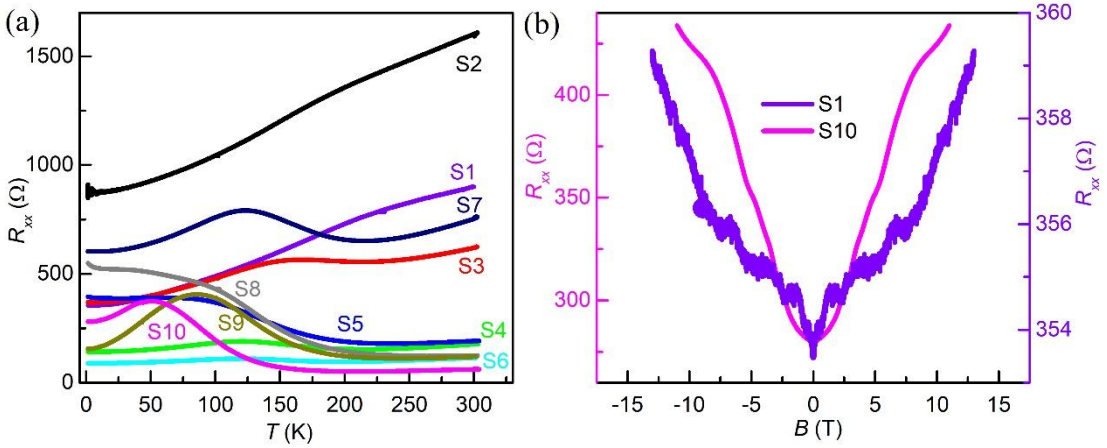

FIG. S5. Temperature and magnetic field dependence of longitudinal resistance for samples with different thickness. (a) Temperature dependence of longitudinal resistance for sample S1 to sample S10 in table I. (b) In-plane perpendicular magnetic field dependence of longitudinal resistance for sample S1 and sample S10. The NLMR effect disappears in both samples.